C. R. Geoscience 350 (2018) 212–221

Contents lists available at ScienceDirect

Comptes Rendus Geoscience

www.sciencedirect.com

Stratigraphy, Sedimentology

Carbonate mounds of the Moroccan Mediterranean margin: Facies and environmental controls

Loubna Terhzaz [a,*], Naima Hamoumi [a], Silvia Spezzaferri [b], El Mostapha Lotfi [c], Jean-Pierre Henriet [d,1]

[a] Group of research ODYSSEE, Materials Nanotechnologies and Environment Laboratory (LMNE), Materials Sciences Research Center, Faculty of Sciences of Rabat, Mohammed-V University Rabat, BP 1014 Rabat, Morocco
[b] Department of Geosciences, University of Fribourg, 1700 Fribourg, Switzerland
[c] ENSET, Mohammed-V University of Rabat, BP 6207 Rabat, Morocco
[d] Department of Geology & Soil Science, Ghent University, 9000 Ghent, Belgium

ARTICLE INFO

Article history:
Received 27 March 2018
Accepted after revision 28 April 2018
Available online 24 June 2018

Handled by Sylvie Bourquin

Keywords:
Carbonate mounds
Cold water corals
Sedimentology
Sedimentary geochemistry
Moroccan Mediterranean margin

ABSTRACT

Sedimentological and geochemical studies of boxcores from the Brittlestar Ridge I and Cabliers carbonate mounds, along the Moroccan Mediterranean margin, show that sediments are composed of cold water scleratian corals and micritic mud, muddy micrite or muddy allochem limestone matrix, outlining seven different facies that can be attributed to "cluster reefs". The mixed siliciclastic/carbonate sediments have been derived from both extra- and intrabasinal sources. Extra-basinal sources may be the geological formations outcropping in the Moroccan hinterland and Sahara, the latter including corals and associated bioclasts. Sediments were transported by wind and rivers and redistributed by bottom currents and local upwelling. Our results confirm the role of tectonics in the genesis of these carbonate mounds and reveal that their developments during the Holocene (10.34–0.91 ka BP) was controlled by climatic fluctuations (e.g. Holocene Climate Optimum and Little Ice Age), eustatic sea level change, and hydrodynamic regime.

1. Introduction

The discovery of cold-water carbonate mounds at the European Atlantic margins over the past decades has increased the interest of the scientific community in these ecosystems (Freiwald, 2002). However, some questions are still open concerning the factors controlling their genesis, development and evolution. Along the Moroccan Mediterranean margin, cold-water carbonate mounds were reported in east of Mellila by Comas and Pinheiro (2007), who named this field "Melilla Carbonate Mound Field" and west of Mellila Lo Iacono et al. (2014). These two fields were named by Hebbeln et al. (2015) as "East and West Melilla Cold water coral Province", respectively (Fig. 1). Studies on the eastern Melilla Province mostly focused on descriptions and age determinations of corals and their associated fauna (Fink et al., 2013; Stalder et al., 2015). A geochemical study carried out by Fink et al. (2013) revealed that cold-water corals (CWC) were prolific during the last glacial–interglacial transition (13.5–12.8 ka BP), early Holocene (11.3–9.8 ka BP) and the mid-Holocene (5.4 ka BP) and that their development was controlled by marine productivity and circulation patterns. Fink et al. (2013) also highlighted arid conditions between 16 and 9.6 ka BP with high input of aeolian dust followed by humid conditions between 9.8 and 8 ka with enhanced fluvial input. Furthermore, a sedimentological study by

* Corresponding author.
E-mail addresses: Loubna.terhzaz@gmail.com (L. Terhzaz), naimahamoumi5@gmail.com (N. Hamoumi).
[1] Deceased author.

https://doi.org/10.1016/j.crte.2018.04.003
1631-0713/

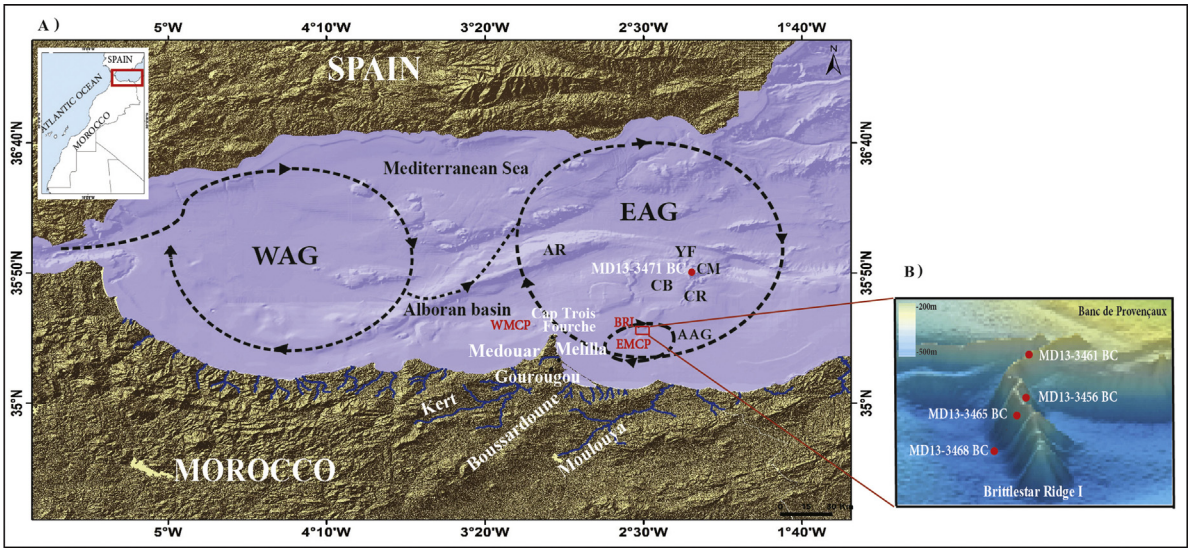

Fig. 1. A. Location of the study area and the boxcore MD13 3471 BC. Topography and bathymetries from the Digital Elevation Models (DEM) and Shuttle Radar Topography Mission (SRTM) of Earth Explorer–USGS source; red square: Brittlestar Ridge I (BRI); WMCP: West Melilla Cold water coral Province; EMCP: East Melilla Cold water coral Province (Comas and Pinheiro, 2007; Hebbeln et al., 2015; Lo Iacono et al., 2014); red point: Cabliers mound (CM) and Boxcores location; AB: Alboran Ridge; CR: Cabliers Ridge; CB: Cabliers Bank; YF: Yusuf Fault; WAG: western Alboran Gyre; EAG: eastern Alboran Gyre; AAG: Atlantic Anticyclonic Gyre (after L'Helguen et al., 2002). B. 3D map of Brittlestar Ridge I, BRI, (Fink et al., 2013) and the location of the studied boxcores.

Titschack et al. (2016) indicates for the upper Unit of the Brittlestar Ridge I (1) that the CWC skeletons represent around 20% of the deposits, (2) that the carbonate content results from organic and detrital sources and (3) that the aggradation rate is between 125 and 241 cm·kyr^{-1}. The aim of this work is to contribute to a better understanding of the formation and evolution of the uppermost part of two carbonate mounds, Brittlestar Ridge I (BRI) and the Cabliers Mound (CM), located along the Moroccan margin, off Melilla (Fig. 1A). In this study, we describe the main sedimentary facies and infer the sediment source and transport mechanisms through grain size, mineralogical and geochemical analyses of the investigated boxcores.

2. Geological and oceanographic settings

2.1. Geological setting

The Moroccan Mediterranean margin consists of a rather narrow continental shelf from 5 to 16 km in width (Tesson and Gensous, 1978). The shelf (Fig. 1) is connected through a steep slope to the southern Alboran basin (1200 m water depth), which presents an irregular topography with ridges, and to the Provençaux and Cabliers Banks (Comas et al., 1999; Fink et al., 2013; Gràcia et al., 2016; Hebbeln et al., 2015). The BRI (Fig. 1) is the steepest and highest of the three existing ridges, it has a sinusoidal shape and reaches 6 km in length and 80 m in elevation from the sea floor (Fink et al., 2013). The CM outcrops in the Cabliers bank, which is bounded by depressions at its eastern and western sides, by a channel, connects to the Yusuf fault at its northern side and is bounded by the Cabliers Ridge to the south (Gràcia et al., 2016). The ridges and most mounds in this region are aligned in deep and large depressions (Comas et al., 1999).

The Moroccan Mediterranean margin is an active margin that develops in a regional compressive context linked to the NW–SE convergence of the Africa and Eurasian plates (Auzende et al., 1975). The Alboran basin originated at the end of the Cretaceous by the thinning of the thick continental crust as a result of the continental collision of the surrounding Betic and Rif Chains (Comas et al., 1999). After the paroxysmal phases of the Alpine orogeny, this hinterland was subjected to compressional and distensional tectonics during the Neogene and Quaternary and was accompanied by a calc-alkaline volcanism (Guillemin and Houzay, 1982; Hernandez, 1983; Louaya and Hamoumi, 2010; Morel, 1989). This tectonic activity is still recorded at present as shown by the numerous earthquakes that affect the region (Vázquez et al., 2014).

2.2. Oceanographic setting

Four water masses have been identified in the Mediterranean Sea (Benzohra and Millot, 1995; Gascard and Richez, 1985; Parilla et al., 1986):

- the Atlantic water, in the upper 150 m of water depth, with a salinity of 36.5 psu increasing up to 38.0 psu while progressing eastward through the Strait of Gibraltar and with a temperature of 16 °C; the characteristics of this water is not regular from west to east;
- the Modified Atlantic Water (MAW), between 150 to 200 m in water depth, with a salinity of 38.3 psu and a temperature ranging from 12.65 to 13.20 °C, flowing through the Strait of Gibraltar into the Algerian basin:
- the Levantine Intermediate Water (LIW), between 200 and 600 m water depth, formed in the eastern Mediterranean and flowing westward to the Atlantic

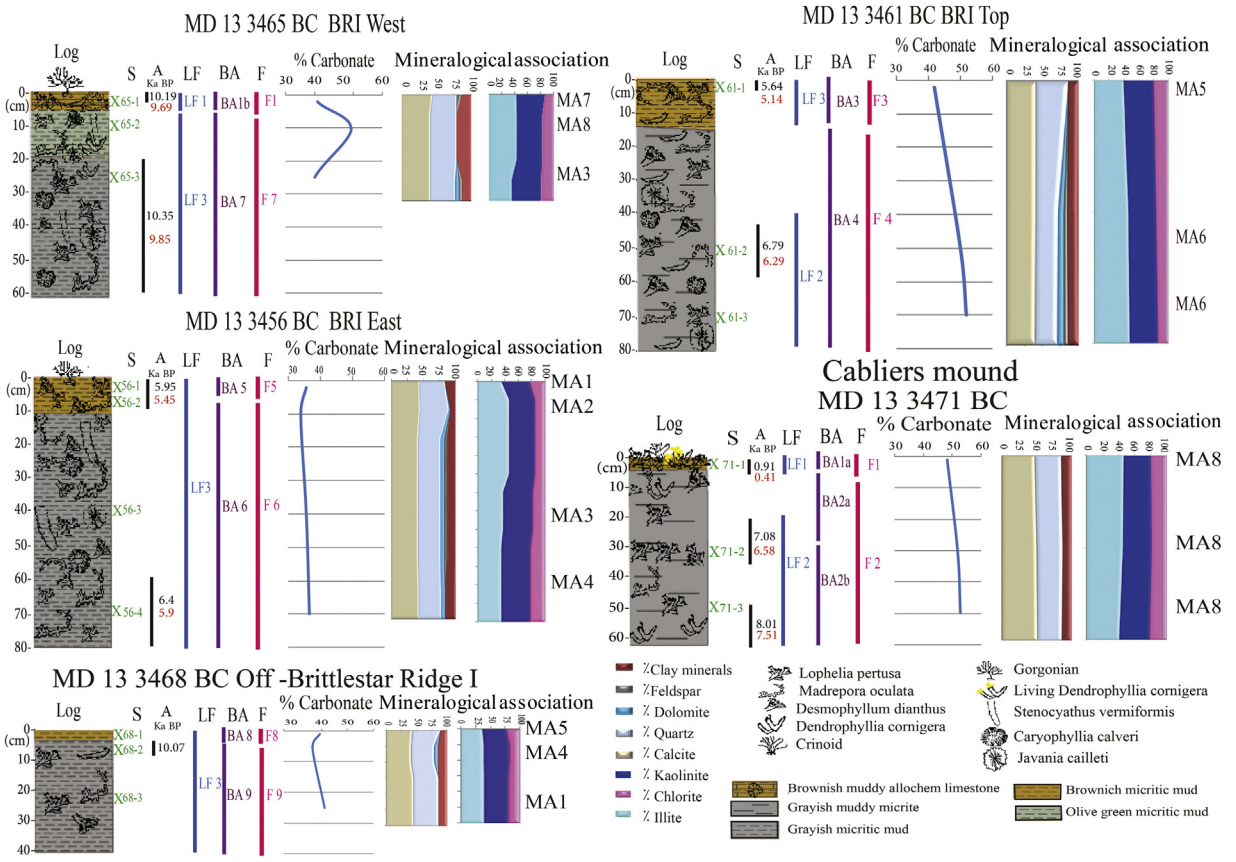

Fig. 2. Sedimentary facies, carbonate contents and mineralogical associations of the sediments from Brittlestar Ridge I and Cabliers Mounds. S: Sample names; X: sample positions; A: Age. Numbers in black: coral age (Schröder-Ritzrau et al., 2015); Numbers in red: estimated sediment age (proposed by Stalder et al., 2015); F: facies; LF: lithofacies; BA: biological assemblage, MA: mineralogical association.

Ocean. The LIW is characterized by a high salinity (> 38.4 psu) and a temperature of ~ 13.15 °C;

- the Western Mediterranean Deep Water (WMDW), found below the LIW, characterized by a salinity of 38.4 psu and a temperature of 12.8 °C.

The circulation of surface water is linked to two anticyclonic gyres of about 100 km in diameter: the Western Alboran Gyre (WAG) and the Eastern Alboran Gyre (EAG) (Fig. 1A), which can reach a water depth between 200 and 300 m (Heburn and La Violette, 1990). Associated with these gyres, eddy structures may develop, such as the Atlantic Anticyclonic Gyre (AAG) (Fig. 1A), which is found above the East Melilla carbonate mound province (L'Helguen et al., 2002).

The temperature decreases from 15 °C to 13.15 °C, and the salinity increases from 36.77 to 38.37 psu, between the surface and a water depth of 200 m (Hebbeln et al., 2015).

3. Materials and methods

The studied boxcores were collected during the EUROFLEETS Gateway cruise (MD 194) on the R/V *Marion-Dufresne* (10–21 June 2013), from carbonate mounds located off Melilla. The following carbonate mounds were sampled: CM (MD13-3471, BC 35°47.74′ N, 2°15.16′ W) at a water depth of 314 m, BRI East (MD13-3456 BC, 35°26.19′ N, 2°30.80′ W) at a water depth of 330 m, BRI Top (MD13-3461 BC, 35°26.53′ N, 2°31.07′ W) at a water depth of 320 m and BRI West (MD13-3465 BC, 35°26.06′ N, 2°30.85′ W) at a water depth of 346 m, and off-BRI (MD13-3468 BC, 35°25.91′ N, 2°30.86′ W) at a water depth of 470 m (Fig. 1A, B). Sixteen samples (Fig. 2) were taken from all lithologies identified following on-board visual core description (Van Rooij et al., 2013). The mineralogical and biogenic composition (mostly the matrix) of the lithofacies was identified using a binocular microscope, its calcium carbonate content measured by calcimetry and grain size determined using the French AFNOR series of sieves (AFNOR-NFX 11-501, 1957). The mineralogical analyses were carried out on bulk samples and clays (< 2 μm) using the X-ray diffractometer of the Technical Support Units for Scientific Research (UATRS) at the National Center of Scientific and Technical Research (CNRST). The semi-quantitative determination of the mineral content is estimated from the integrated intensities of the diffraction peaks (the error rarely exceeds 2%).

The geochemical analysis of major and trace elements (%) was carried out using the X-ray fluorescence spectrometer (error = 0) at the UATRS, CNRST. The obtained data sets were processed using Principal Component Analysis (PCA) and linear regression lines, alteration ratios, and elemental

ratios. The values of the Chemical Index of Alteration $CIA = (Al_2O_3/Al_2O_3 + CaO^* + NaO_2 + K_2O) \times 100$ are applied following Nesbitt and Young (1982) and the Plagioclase Index of Alteration $PIA = (Al_2O_3 - K_2O)/[(Al_2O_3 - K_2O) + CaO^* + Na_2O)] \times 100$ is after Fedo et al. (1995). The alteration ratios $M_1 = (FeO + MgO + Al_2O_3)/(K_2O + NaO + -CaO)$ and $M_2 = Al_2O_3/(FeO + MgO)$ have been calculated and applied following Englund and Jorgensen (1973).

Biological assemblages are derived from the description of the biogenic assemblages (corals and associated sessile and vagile fauna), as identified and described by Vertino (in Van Rooij et al., 2013). The age of the corals was established by Schröder-Ritzrau et al. (2015) using the $^{230}Th/^{234}U$ daughter-deficiency dating method (Fig. 2).

4. Results

4.1. Structure and sedimentary facies

The sediments from the carbonate mounds are composed by matrix and biogenic components consisting of corals and associated fauna. Therefore, their facies are defined based on their lithofacies and biological assemblages.

4.1.1. Biological assemblages

The corals consist of cold-water scleratinians corals with predominant *Madrepora oculata, Desmophyllum dianthus*, *Dendrophyllia cornigera*, and *Lophelia pertusa*, accompanied by less abundant solitary corals *Caryophyllia calveri*, *Javania cailleti*, and *Stenocyathus vermiformis*. The age of the corals ranges between 0.91 and 10.35 ka BP according to Schröder-Ritzrau et al. (2015) (Fig. 2). With the exception of the top of CM, where live scleractinians were collected (one specimen of *D. cornigera* and tiny *D. dianthus* polyps), all recovered corals were dead and fragmented. Some of them were exposed on the seafloor but, in most cases, they were embedded in the fine-grained matrix (Fig. 2). The corals show different degrees of preservation, from well-preserved to bio-eroded and degraded and sometimes are covered with black ferruginous crusts. Nine biological assemblages (BA1 to BA9) including four sub-biological assemblages (BA1a, BA1b and BA2a, BA2b) were identified (Fig. 2) based on corals assemblages and the associated biota were described by Vertino in Van Rooij et al. (2013,supplementary data S1). The off-BRI biological assemblages are distinctly different from the others, the BA9 contains a few fragments of reworked *L. pertusa* and *M. oculate*, whereas BA8 shows no corals.

4.1.2. Lithofacies

The microscopic studies revealed a biogenic fraction composed of foraminifera, tiny coral fragments and other calcareous bioclasts of sizes ranging from the μm to the mm scales, together with siliciclastic components (e.g. quartz, feldspars and clay). The calcium carbonate content, measured from mound matrix, varies from 34 to 53% (Fig. 2). The highest values are recorded at the CM. At all sites, the carbonate contents are higher in sediments at the base of the boxcore than at its top, except in the West BRI. They vary from 53% to 48% in CM, 37% to 36% in BRI East, 52% to 42% in BRI Top and 40% to 41% in BRI West. Off-BRI, the values range from 41% to 39%. The grain size analyses show that the sediments associated with the BRI and CMs are dominated by the very fine fraction (< 45 μm) and that the fine sand fraction does not exceed 3%. Three lithofacies (LF) are recognized, composed of mixed (siliciclastic/carbonate) sediments corresponding in the Mount's classification (Mount, 1985) to a muddy allochem limestone (LF1), a muddy micrite (LF2), and a micritic mud (LF3) (Fig. 2).

4.1.3. Facies

All nine facies (F) are recognized based on the assemblage of lithofacies and biological assemblage (Fig. 2 and Supplementary Data S1). Facies F1 to F7 correspond to the "skeletal mound type" in the classification of James and Bourque (1992). They are composed of dominant matrix and corals in place but never in contact, thus the mounds are considered as "cluster reef" following Riding (2002). Facies F8 and F9, which characterized the sediments off-BRI, correspond to off-mound deposits, no corals are observed in F8 and F9 contains a few reworked fragments of coral.

4.2. Mineralogical composition

X-ray diffractometry of bulk sediments and clay fractions reflects eight mineralogical associations (MA1 to MA8, Fig. 2), in which the ubiquitous minerals are: calcite, quartz, kaolinite, illite and chlorite. The differences among mineral associations can be summarized as follows: 1) predominance of calcite on quartz in MA1, MA3, MA4, MA6, MA7 and MA8, 2) presence of dolomite in MA2, MA3, MA4 and MA6, 3) presence of feldspar in MA3 and MA6 and 4) predominance of kaolinite on illite in MA1, MA3, MA4, MA5 and MA7. These mineralogical associations imply the existence of carbonate and siliciclastic source components.

4.3. Geochemistry

4.3.1. Sediment sources

Sediments were characterized using principal component analyses (PCA) of the major elements and correlation between the major elements. The PCA of major elements (Fig. 3) allows one to highlight geochemical signatures characterizing three sediment sources: a biogenic source for lithofacies LF1 and LF2 of CM and for LF1 of BRI West, a terrigenous source for LF3 of BRI East and off-BRI and a mixed source (terrigenous/biogenic) for LF3 and LF2 of BR I Top, and LF3 off-BRI.

The correlations between the major elements allow one to characterize the source of some minerals. The negative correlation between MgO and LOI (loss on ignition) suggests that MgO is of detrital origin (Fig. 4A). The zero to low positive correlation between P_2O_5 and CaO and between P_2O_5 and LOI indicates a mixed organic and mineral origin (Fig. 4B, C). The strong negative correlation between CaO and Al_2O_3 of ($R^2 = 0.652$) reflects a marine

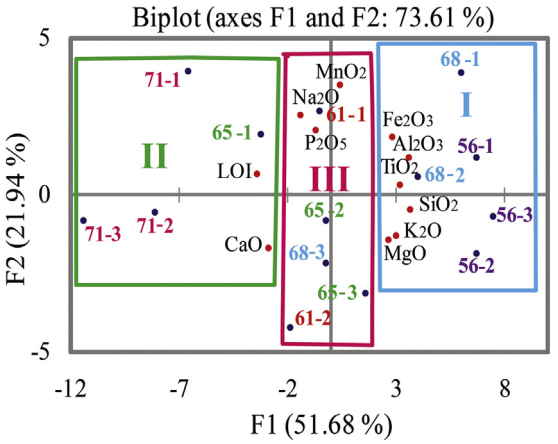

Fig. 3. Principal component analyses, variables, and samples in the axes F1 and F2. I: Terrigenous signature, II: biogenic signature, III: mixed signature (terrigenous + biogenic).

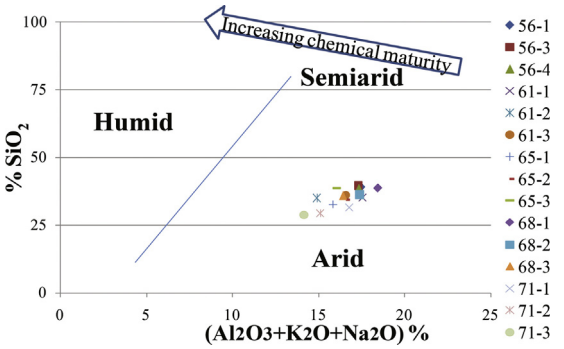

Fig. 5. $\%SiO_2/\%(Al_2O_3 + K_2O + Na_2O)$ rates of samples plotted in the diagram of Suttner and Dutta (1986).

origin for a large part of Ca (Fig. 4D). The strong positive correlation of SiO_2 and TiO_2 with Al_2O_3 indicates that the quartz is not related to remains of siliceous organisms (Fig. 4E, F).

4.3.2. Climatic controls

The binary diagram $(\%SiO_2/\%(Al_2O_3 + K_2O + Na_2O)$ proposed by Suttner and Dutta (1986) shows that the siliciclastic sediments of CM and BRI were deposited under arid climatic conditions (Fig. 5).

4.3.3. Evaluation of the chemical maturity

The values of the Chemical Index of Alteration CIA (Nesbitt and Young, 1982) and the Plagioclase Index of Alteration PIA (Fedo et al., 1995), vary from 58.54 to 70.26 and from 59.58 to 73.82, respectively. However, most samples have a value above 60, which indicates a moderate degree of alteration in the source zone and an average destruction of the feldspar during transport and sedimentation. The lowest CIA values were found at the surface sediment of CM (58.54) and the BRI Top (59.18). Furthermore, the alteration ratios M1 and M2 (See Section 3) vary between 0.75 and 1.52 and between 2 and 2.33, respectively. Those values, plotted in the triangular diagram of Englund and Jorgensen (1973) (Fig. 6) show that the studied samples fit in the A1 class and reflect unaltered sediments.

4.3.4. Transport modes

The plots of the K/Al, Mg/Al, Rb/Al, Si/Al, Ti/Al and Zr/Al ratios indicate two modes of terrigenous sediment transport towards the study area: fluvial and aeolian (Fig. 7) (Calvert and Pedersen, 2007; Jimenez Espejo et al., 2007). Ti and Zr can be derived from heavy-minerals (e.g. rutile and zircon) and Si from quartz contained in North African dust. Increases in Ti/Al, Zr/Al and Si/Al ratios

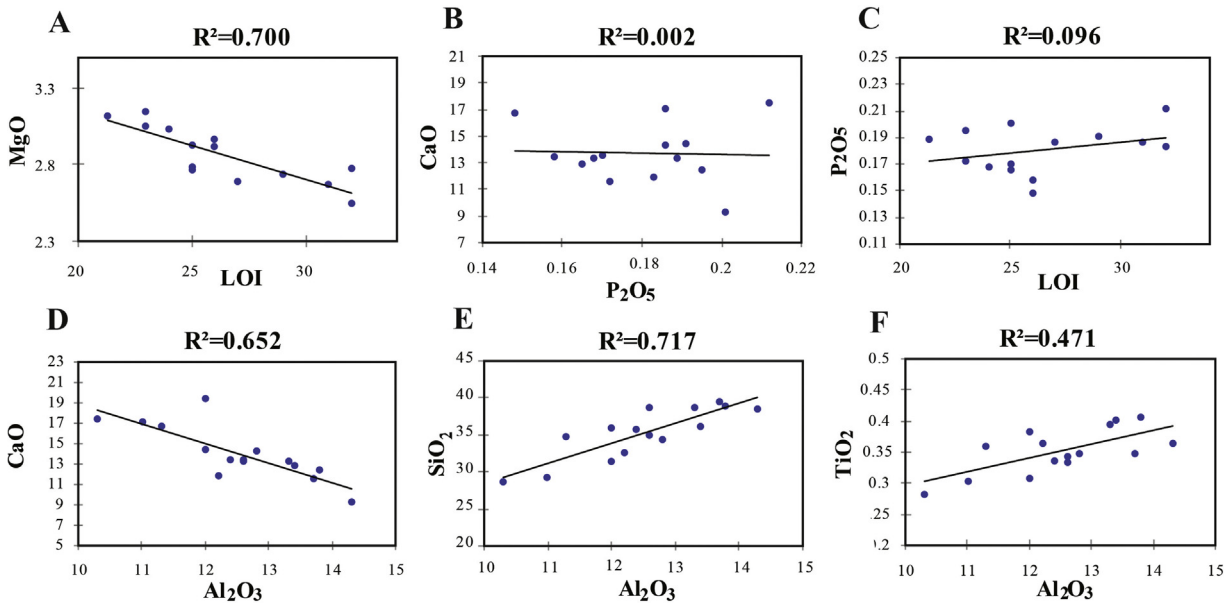

Fig. 4. Correlations between the major elements.

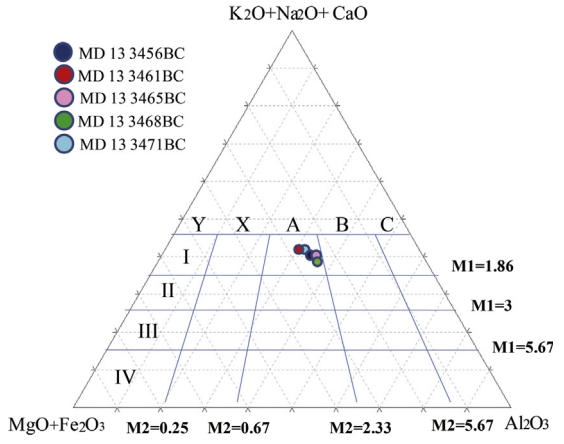

Fig. 6. Alteration rates of the samples plotted in the diagram of Englund and Jorgensen (1973).

suggest increased aeolian supply (e.g. Calvert and Pedersen, 2007). Moreover, the opposite trend of the Zr/Al ratio against the Si/Al ratio towards the top of CM (Fig. 7) may indicate either a different source area and/or varying sensitivities to wind speed (e.g. Jimenez Espejo et al., 2007). Mg is linked to clays and especially to a possible chlorite-rich source; it may be also related to dolomite (e.g. Jimenez Espejo et al., 2007). Rb can replace K in aluminosilicate minerals and is abundant in micas; the K/Al ratio may therefore reflect an increase in the relative proportions of kaolinite relative to illite (e.g. Calvert and Pedersen, 2007), when local rivers (e.g. the Moulouya River) supplied more kaolinite to the basin. The data furthermore allow us to qualify the dominance of each of these modes of transport in space and time.

5. Discussion: evolution and control of carbonate mounds

The development of CM and BRI results from the interaction of growth phases of cold-water corals, erosion and sedimentation processes. Corals proliferated during the Pleistocene–Holocene transition at 10.35 ka, 10.19 ka, 10.07 ka and in the Holocene at 8.01 ka, 7.08 ka, 6.79 ka, 6.4 ka, 5.95 ka and 0.91 ka BP (Fink et al., 2013; Schröder-Ritzrau et al., 2015; Stalder et al., 2015). According to Riding (2002), the accumulation of sediments promotes the rapid growth of corals (constructors), which in turn act as traps for sediments. These sediments are composed of a carbonate phase (calcite and dolomite) and a siliciclastic phase. The calcite could have been derived from bioerosion and disintegration of corals and other bioclasts. The presence of a biogenic source is demonstrated by: (1)

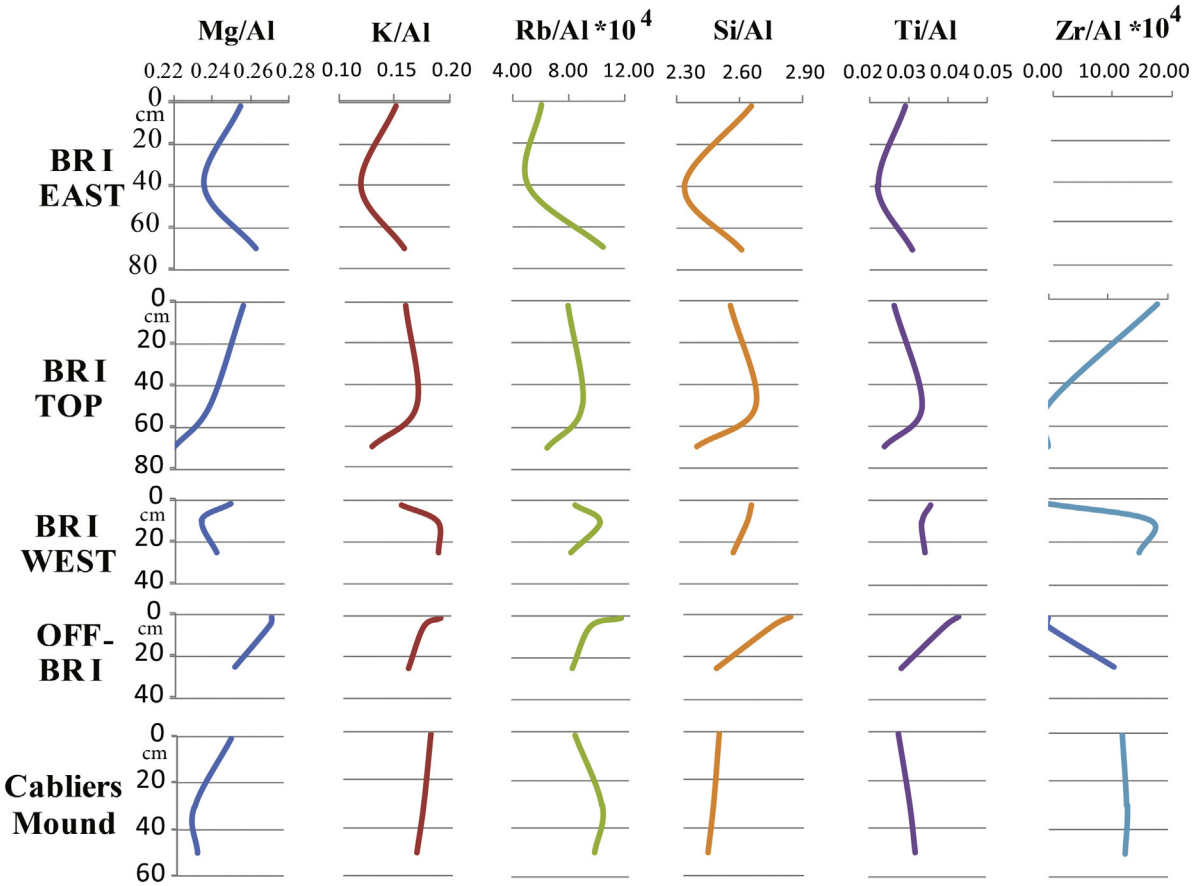

Fig. 7. Trace and major elements in relation to Al (BR I: Brittlestar Ridge I).

the great amount of bioclasts (especially in LF1), (2) by the highlighting of biogenic and mixed sources through principal component analyses and (3) by the zero to weakly positive correlation between P_2O_5 and CaO (Fig. 4B), reflecting a mixed origin (organic and mineral) and (4) by the strong negative correlation between CaO and Al_2O_3, which reflects a marine origin for the greater part of the $CaCO_3$ (Fig. 4D). However, a part of the calcite is of detrital origin and would be supplied together with dolomite and siliciclastic components from the geological formations of the Moroccan hinterland and the Sahara. This is corroborated: (1) by the mineralogical associations (Fig. 2), which are similar to those of the geological formations in the hinterland (Mahjoubi et al., 2003) and the Moroccan Alboran margin (El Moumni, 1987) and (2) by the detrital origin of dolomite, as indicated by the negative correlation between MgO and LOI (Fig. 4A) and because dolomite is part of sediments derived from terrigenous or mixed terrigenous/biogenic sources and results from high or relatively moderate fluvial supply. The strong positive correlation of SiO_2 and TiO_2 with Al_2O_3 indicates that the quartz is not related to a biogenic source (Fig. 4E, F) and that the high quartz content characterizing the sediments results from a high continental input (Fig. 7). Feldspar is present only in some levels of BR I (Fig. 2) and associated with deposits having either a terrigenous or a mixed source. It has been derived either from the erosion of the volcanic formations of the hinterland or from volcanic eruptions of Cap des Trois Fourches and Gourougou (Hernandez, 1983) (Fig. 1).

The siliciclastic sediments of CM and BRI were deposited under arid climate conditions, as shown in the binary diagram (Fig. 5) and by their moderate to weak chemical weathering (Fig. 6). Their transport from the hinterland was provided by winds and input through fluvial currents, as demonstrated by their chemical ratios (Fig. 7) and the relatively high values of Zr/Al in CM. Zr/Al ratios between 12 and 19 were also reported by Martín-Puertas et al. (2010) and Nieto-Moreno et al. (2011) to indicate higher aeolian supply from the Sahara prior to 2.7 ka and in the western Mediterranean region during the Little Ice age. The correlation of the transport mode with rainfall variability, as proposed by Wengler et al. (1992) for the Rharbian (Holocene), shows that high and moderate fluvial supplies in BRI (which is closer to the mainland–around 35 km) may coincide with a semi-arid and sub-humid climate with an average of 520–600 mm rainfall per year. Fluvial transport in such a period was favored by torrential flows of the Kert, Medouar, Boussardoune and Moulouya Rivers (Louaya and Hamoumi, 2006, 2010), debouching into the Mediterranean (Fig. 1). Enhanced fluvial supply was also demonstrated by Fink et al. (2013) in the EMCP off mound record during the late Holocene. High aeolian supply in CM (which is about 75 km from the mainland) coincides with an arid climate (380 mm rainfall per year) and a semi-arid climate (average of 400–550 mm of rainfall per year).

The composition of the lithofacies and biological assemblage, as well as the characteristics of the carbonate mounds of the CM and BRI, were modulated by climate oscillations of decadal to centennial scale of the Holocene interglacial stage: warm/cold, reported by Dansgaard et al. (1969) and Schönwiese (1995) and cycles of humidity/aridity, proposed by Wengler et al. (1992).

The reconstruction of the climates that controlled the development of carbonate mounds is based on coral and sediment ages (Schröder-Ritzrau et al., 2015), taking into account the interval of 500 years between the age of corals and the matrix sediments proposed by Stalder et al. (2015). The CM is composed from base to top by muddy micrite (LF2) and muddy allochem limestone (LF1). The siliciclastic input here was provided by high aeolian and moderate fluviatile supplies, during a semi-arid climate with 400–550 mm rainfall per year for LF2 ($\sim$ 7.51 and $\sim$ 6.58 ka) and an arid climate with 380 mm rainfall per year for LF1 ($\sim$ 0.41 ka). The carbonate phase is essentially derived from a biogenic source. The high carbonate contents and the presence of shell fragments of vagile and sessile epifauna are most likely related to the degradation and disintegration of carbonate after a mass death of local mound fauna, probably in relation to warming. Indeed, the sedimentation on this mound coincides for LF1 with a warming period after the Little Ice age, with temperatures of around 15.5 °C. LF2 coincides with a warming period related to the Holocene Climate Optimum (6.2–7.8 ka). Sediments from BR I East mound are composed of micritic muds (LF3), which are correlated to terrigenous sources in the Moroccan hinterland. Deposition was produced from high or moderate fluvial and low aeolian supply between semi-arid and sub-humid climate period with rainfall of 600–610 mm per year. Sedimentation took place between $\sim$ 5.9 and 5.45 ka. Sediments at the BR I top consist of muddy micrites (LF2) topped by micritic mud (LF3) derived from a mixed (terrigenous/biogenic) source. LF2 (dated at $\sim$ 6.29 ka) is fed by moderate fluvial and a low aeolian supply during a semi-arid climatic period, with an average rainfall of $\sim$ 560 mm rainfall per year. The formation of LF2 took place during the Holocene Climate Optimum (15.9 °C). LF3 ($\sim$ 5.14 ka) is characterized by high fluvial and high aeolian supplies between semi-arid and sub-humid climatic periods, with 600 mm of rainfall per year. Sediments at BRI I West are composed of micritic mud (LF3) from a mixed source (terrigenous/biogenic) topped by muddy allochem limestone (LF1) derived from a biogenic source. LF3 ($\sim$ 9.85 ka) is supplied by relatively high aeolian and moderate fluvial inputs, in contrast to LF1 ($\sim$ 9.69 ka) which is fed by moderate fluvial and low aeolian supplies. They both coincide with a semi-arid climate with 510–520 mm of rainfall. Sedimentation of LF1 took place during the deglaciation stage at the beginning of the Holocene at $\sim$ 9.69 ka for LF1 (14.7 °C) and at $\sim$ 9.85 ka for LF3 (14.6 °C). Sediments off mound-BRI consist of micritic mud (LF3). Here its basal deposits are derived from a mixed source with relatively high aeolian and moderate fluvial supplies. The muds of the (LF3) level (dated at 10.07 ka, Schröder-Ritzrau et al., 2015) up to the surface are derived from a terrigenous source with high fluvial and low aeolian supplies. These off-mound deposits include also sediments and corals from the carbonate mounds that probably slid along the slope of the ridge.

The cold-water corals ecosystems of the Moroccan Mediterranean margin, like those of the Strait of Gibraltar and the Moroccan Atlantic margin, were initiated during the Last Ice age (Fink et al., 2013; Hamoumi, 1997; Wienberg et al., 2009). Corals from the Melilla Province proliferated during the Pleistocene–Holocene transition (Fink et al., 2013; Stalder et al., 2015). Only part of the biological assemblages BA1a and BA1b is characterized by the same coral species, all other biological assemblage containing different species. All studied mounds are characterized by two distinct biological assemblages (Fig. 2). These variations appear to be controlled by climate changes during the Holocene, as demonstrated by the correlation between the biological assemblage and variations of near-surface temperatures in the Northern Hemisphere during the last 11,000 years (Dansgaard et al., 1969; Schönwiese, 1995), taking into account that the temperature of seawater decreases with depth, from 15 °C to 13.15 °C between the surface and 200 m (Hebbeln et al., 2015). The biological assemblage showing the greatest diversity, density and size of corals as well as the presence of a more diverse and larger associated fauna reflects the coldest conditions, with temperatures below 13 °C. Nevertheless, when temperatures are above 15 °C, cold-water corals are rare and small. However, although the majority of cold-water corals requires temperature conditions between 4 °C and 13 °C (Freiwald, 2002), *L. pertusa* and *M. oculata* can live at temperatures ranging from 5 °C in the North Atlantic Ocean to 13.9 °C in the Mediterranean Sea, and *D. cornigera* is less sensitive to temperature increase. According to Gori et al. (2014), *D. cornigera* can live between 12 and 16 °C. *Madrepora oculata* and in particular, *Dendrophylliidae* have a higher tolerance to temperature changes than *L. pertusa*.

This biodiversity could also be favored by oceanographic conditions and increased nutrient inputs in the Alboran Sea. The ridges as well as most mounds in the East Melilla province are surrounded by wide and deep depressions with strong bottom currents (Comas et al., 1999), especially around the BRI. The effect of long-lasting bottom currents, reinforced by topography, is observed in several sites in the Alboran Sea (Hernández-Molina et al., 2011). These currents prevent corals from burial by sediments and promote additional nutrient flows relayed by ascending currents, thus creating a favorable environment for development of a high diverse fauna. Upwelling has been recognized in the northwestern Alboran Sea (Sarhan et al., 2000); where the westerly winds trigger the upwelling of nutrient-rich deep waters, leading to enhanced biological productivity rates of up to 200 $g{\cdot}C{\cdot}m^{-2}{\cdot}yr^{-1}$ (Sarhan et al., 2000). Today upwelling has also been observed along the Algerian coasts (Bakun and Agostini, 2001) and along the Almeria–Oran frontal zone, with high primary productivity in relation to the density front created by the difference in salinity between Atlantic waters and the Mediterranean surface waters (Prieur and Sournia, 1994). These zones of high productivity and transport of biogenic material into the gyres are shown in satellite images reflecting increased concentrations of chlorophyll *a* (0.21 to 0.67 mg/m^3) (Baldacci et al., 2001). The on-set of new oceanographic conditions in the Mediterranean Sea at about 8 ka BP accompanied by the deepening of the pycnocline and the reinforcement of nutrient input between the Atlantic and the Mediterranean water was reported by Rohling et al. (1995) based on planktonic foraminifera. Benthic foraminifera from the Melilla carbonate mound province (Stalder et al., 2015) indicate nutrient-rich, well-oxygenated and relatively high-energy currents with strong seasonal plankton blooms between 10 ka and 6 ka.

The East Melilla carbonate mound province belongs to an active margin, whose NW–SE convergence has been reactivated during the Upper Tortonian and Quaternary (Guillemin and Houzay, 1982; Louaya and Hamoumi, 2010; Morel, 1989). Tectonic control thus has also played a major role in the initiation and the development of the corals by shaping an irregular topography and forming a hard substratum. The banks and ridges outcropping in this province probably uplifted following transtensive and transpressive tectonics during the Holocene (Comas et al., 1999). Morphological highs (ridges, mud volcanoes and banks), have formed favorable habitats at water depths of around 200–300 m. In addition, a relationship between carbonate mounds and deep fluids could be supported by the presence of ferruginous crusts covering some coral fragments in CM and BRI. These encrustations are similar to the iron and manganese coating on fossil coral fragments (tubotomaculum) associated with the mud volcano deposits in the western Rif, which were interpreted as the result of precipitation of Fe and Mn in relation to hydrothermal circulations induced by mud volcanism (Hamoumi, 2005). Mud volcanoes have been recognized along the Moroccan Mediterranean margin (Comas and Pinheiro, 2007) and the association of cold-water corals with mud volcanoes has been reported from the Moroccan Mediterranean margin (Margreth et al., 2011) and the Gulf of Cadiz (Foubert et al., 2008).

The Holocene period is marked by eustatic variations in the Mediterranean Sea, induced by a combination of climatic changes and tectonics. The first eustatic sea level rise is related to the warming at the beginning of the Holocene at 8000 years BP. This was followed by sea level rises at: 7570 years BP, 7000 years BP, 6000 years BP, 5900 years BP, 5500 years BP, 4800–4500 years BP and 3500–3300 years BP (Aloisi et al., 1978; Blázquez et al., 2017). The ages of corals from the CM and BRI mounds are consistent with periods of high sea level, suggesting an eustatic control on coral evolution. This has also been demonstrated in the Strait of Gibraltar (Hamoumi, 1997) and the Alboran Moroccan margin (Fink et al., 2013; Lo Iacono et al., 2014; Stalder et al., 2015).

6. Conclusion

Sedimentological and geochemical studies of the Brittlestar Ridge I and the Cabliers carbonate Mound of the East Melilla province in the Moroccan Mediterranean margin allows one to distinguish sedimentary facies, sedimentary sources, modes of sediment transport and the genesis and control of the mounds. These mounds are of "cluster reef" type sensu Riding (2002) and are characterized by cold-water scleractinian corals dominated by *M. oculata, D. dianthus.*

D. cornigera, and *L. pertusa*, accompanied by *C. calveri*, *J. cailleti*, and *S. vermiformis*, as well as have a diverse sessile and vagile fauna and a dominant matrix of micritic mud, muddy micrite and muddy allochem limestone. Part of the carbonate matrix is derived from bioerosion and degradation of corals, skeletons and shells, as well as chemical precipitation and microbiological processes. The other part of the matrix and the siliciclastic components has been derived from geological formations of the Moroccan hinterland and Sahara through transport by winds and rivers and in the sea by bottom currents and upwelling of nutrient-rich water. Sediments at the Cabliers Mound (located far from the mainland) are from a biogenic source with a small terrigenous component transported by winds. The Brittlestar Ridge I is closer to the mainland and sedimentation here is of terrigenous or mixed (terrigenous/biogenic) origin, with high terrigenous input dominated by fluvial transport.

The development, genesis, and evolution of carbonate mounds in the studied areas is controlled by tectonics, climate, eustasy and hydrodynamic regime. Tectonics played a major role in forming the irregular topography and hard substrate with shoals (ridges, mud volcanoes and banks) at water depths ranging from 200 to 300 m. These structures are relatively far away from terrigenous inputs, but the action of bottoms currents and upwelling of nutrient-rich waters have created favorable habitats for cold-water corals. Climatic fluctuations during the Holocene (e.g. Holocene Climate Optimum and Little Ice Age) triggered the oceanographic conditions and the hydrodynamic regime that controlled the sedimentation in the area.

Acknowledgements

Thanks are due to Dr. David Van Rooij for giving us the opportunity to participate in the MD 194 cruise onboard the research vessel *Marion-Dufresne*, to Dr. Agostina Vertino for the determination of the coral species, to Dr. Francisca Martinez Ruiz and to Dr. Tjeerd Van Weering for their insightful comments and suggestions, as well as for the time devoted to the correction of this paper, and to Dr. Sylvie Bourquin for the pertinent remarks and the efforts provided to publish this paper.

Appendix A. Supplementary data

Supplementary data associated with this article can be found, in the online version, at https://doi.org.10.1016/j.crte.2018.04.003.

References

AFNOR-NFX 11-501, 1957. Woven wire test sieves. .

Aloisi, J.-C., Monaco, A., Planchais, N., Thommeret, J., 1978. The Holocene transgression in the Golfe du Lion, southeast France: paleogeographic and paleobotanical evolution. Geogr. Phys. Quat. XXXII (2), 145–162.

Auzende, J.-M., Bonnin, J., Olivier, J.-L., 1975. La marge nord-africaine considérée comme une marge active. Bull. Soc. geol. France 17 (4), 486–495.

Bakun, A., Agostini, V.N., 2001. Seasonal patterns of wind induced upwelling/downwelling in the Mediterranean Sea. Sci. Mar. 65 (3), 243–257.

Baldacci, A.G.C., Grasso, R., Manzella, G., et al., 2001. A study of the Alboran sea mesoscale system by means of empirical orthogonal function decomposition of satellite data. J. Mar. Syst. 29, 293–311.

Benzohra, M., Millot, C., 1995. Characteristics and circulation of the surface and intermediate water masses off Algeria. Deep Sea Res. Part I Oceanogr. Res. Pap. 42 (10), 1803–1830.

Blázquez, A.M., Rodríguez-Pérez, A., Torres, T., Ortiz, J.E., 2017. Evidence for Holocene sea level and climate change from Almenara marsh (western Mediterranean). Quat. Res. 88, 206–222.

Calvert, S.E., Pedersen, T.F., 2007. Elemental proxies for palaeoclimatic and palaeoceanographic variability in marine sediments: interpretation and application. In: Hillaire-Marcel, C., Vernal, A.D. (Eds.), Proxies in Late Cenozoic Paleoceanography. Elsevier, Amsterdam.

Comas, M., Pinheiro, L.M., 2007. Discovery of carbonate mounds in the Alboran Sea: the Melilla mound field. Abstract for the First MAPG International Convention, Conference & Exhibition Marrakech Convention Center. 28–31.

Comas, M., Platt, J.P., Soto, J.I., Watts, A.B., 1999. The origin and Tectonic History of the Alboran Bas. Insights from Leg 161 Results. Proc. Ocean Drilling Program Sci. Results 161, 555–580.

Dansgaard, W., Johnsen, S.J., Møller, J., Langway, J.C., 1969. One Thousand Centuries of Climatic Record from Camp Century on the Greenland Ice Sheet. Science 166 (3903), 377–380.

El Moumni, B., 1987. La sédimentation, au Quaternaire terminal, dans la partie méridionale de la mer d'Alboran (Marge marocaine). Thèse de 3e cycle. Université de Perpignan, France (212 p).

Englund, J.O., Jorgensen, P., 1973. A chemical classification system for argillaceous sediments and factors affecting their composition. Geol. Fören. Stockholm Förh. 95 I (1), 87–97.

Fedo, C., Nesbitt, H.W., Young, G.M., 1995. Unraveling the effects of potassium metasomatism in sedimentary rocks and paleosols, with implications for paleoweathering conditions and provenance. Geology 23 (10), 921.

Fink, H.G., Wienberg, C., De Pol Holz, R., Wintersteller, P., Hebbeln, D., 2013. Cold water coral growth in the Alboran Sea related to high productivity during the Late Pleistocene and Holocene. Mar. Geol. 339, 71–82.

Foubert, A., Depreiter, D., Beck, T., Maignien, L., Pannemans, B., Frank, N., Blamart, D., Henriet, J.P., 2008. Carbonate mounds in a mud volcano province off north-west Morocco: Key to processes and controls. Mar. Geol. 248, 74–96.

Freiwald, A., 2002. Reef forming cold water corals. In: Wefer, G., Billett, D., Hebbeln, D., Jørgensen, B.B., Schlüter, M., Van Weering, T. (Eds.), Ocean Margin Systems. Springer-Verlag, Berlin, Heidelberg, pp. 365–385.

Gascard, J.C., Richez, C., 1985. Water Masses and Circulation in the Western Alboran Sea and in the Straits of Gibraltar. Prog. Oceanogr. 15, 157–216.

Gori, A., Reynaud, S., Orejas, C., Gili, J.M., Ferrier Page, C., 2014. Physiological performance of the cold water coral dendrophyllia cornigera reveals its preference for temperate environments. Coral Reefs 33, 665–674.

Gràcia, E., Perea, H., Bartolome, R., Lo Iacono, C., Costa, S., Diez, S., Placaud, X., Smith, C., Rodriguez, P., Sanchez, H., Quedec, O., Danobeitia, J., cruise team, SHAKE., 2016. First AUV and ROV investigation of seismogenic faults in the Alboran Sea Western Mediterranean. Seventh International Workshop on Marine Technology–Martech, Barcelona, Spain.

Guillemin, M., Houzay, J.-P., 1982. Le Néogène post nappes et le Quaternaire du Rif nord-oriental, Maroc. Stratigraphie et tectonique des bassins de Melilla, du Kert, de Boudinar et du piémont des Kebdana. Notes et Mem. Serv. Geol. Maroc 314, 7–238.

Hamoumi, N., 1997. Les formations coralliaires du détroit de Gibraltar: Impact sur le projet Liaison fixe Europe–Afrique par un tunnel, rapport SNED. , 22 p.

Hamoumi, N., 2005. The mud volcanic provinces of the Gulf of Cadiz Moroccan margin and NW Rif belt: challenging areas to better understand complex marine land at a regional scale., 29, CIESM Workshop Monographs, Monaco, pp. 79–85.

Hebbeln, D., Wienberg, C., Bartels, M., Bergenthal, M., Frank, N., Gaide, S., Henriet, J.P., Kaszemeik, K., Klar, S., Klein, T., Krengel, T., Kuhnert, M., Meyer Schack, B., Noorlander, C., Reuter, M., Rosiak, U., Schmidt, W., Seeba, H., Seiter, C., Stange, N., Terhzaz, L., Van Rooij, D., 2015. MoccoMeBo: Climate driven development of Moroccan cold water coral mounds revealed by MeBo drilling Atlantic vs. Mediterranean settings, Cruise MSM36–February 18–March 17, 2014–Malaga Spain–Las Palmas Spain. MARIA S. MERIAN Berichte, MSM36. DFG Senatskommission fuer Ozeanographie. (81).

Heburn, G.W., La Violette, P.E., 1990. Variations in the Structure of the Anticyclonic Gyres Found in the Alboran Sea. J. Geophys. Res.: Oceans 95, 1599–1613.

Hernandez, J., 1983. Le volcanisme miocène du Rif oriental Maroc: Géologie, pétrologie et minéralogie d'une province shoshonitique, Thèse d'État. Université Paris-6, France (458).

Hernández-Molina, F.J., Serra, N., Stow, D.A.V., Llave, E., Ercilla, G., Van Rooij, D., 2011. Along slope oceanographic processes and sedimentary products around the Iberian margin. Geo-Mar. Lett. 31, 315–341.

James, N.P., Bourque, P.A., 1992. Reefs and mounds. In: Walker, R.G., James, N.P. (Eds.), Facies Models, Response to Sea Level Change. pp. 323–347.

Jimenez Espejo, F.J., Martinez Ruiz, F., Sakamoto, T., Iijima, K., Gallego Torres, D., Harada, N., 2007. Paleoenvironmental Changes in the Western Mediterranean since the Last Glacial Maximum: High Resolution Multiproxy Record from the Algero–Balearic Basin. Palaeo3 246 (2), 292–306.

L'Helguen, S., Le Corre, P., Madec, C., Morin, P., 2002. New and regenerated production in the Almeria Oran front area, eastern Alboran Sea. Deep Sea Res. Part I: Oceanogr. Res. Pap. 49 (1), 83–99.

Lo Iacono, C., Gràcia, E., Ranero, C.R., Emelianov, M., Huvenne, V.A.I., Bartolomé, R., BoothRea, G., Prades, J., 2014. The West Melilla Cold Water Coral Mounds, Eastern Alboran Sea: Morphological Characterization and Environmental Context. Deep Sea Res. Part II Top. Stud. Oceanogr. 99, 316–326.

Louaya, A., Hamoumi, N., 2006. Application de la télédétection à l'étude de la géomorphologie et de la morphodynamique du complexe lagunaire de Nador. Bull. Geo. Observateur 15, 51–65.

Louaya, A., Hamoumi, N., 2010. Étude morphostructurale de la région de Nador, Maroc nord-oriental. Afr. Geosci. Rev. 17 (2), 107–127.

Mahjoubi, R., Kamel, S., El Moumni, B., Noack, Y., Parron, C., 2003. Nature, origine and répartition de la phase argileuse de la lagune de Nador Maroc Nord Oriental. Geol. Belg. 6 (1–2), 31–42.

Margreth, S., Gennari, G., Rüggeberg, A., Comas, M.C., Pinheiro, L.M., Spezzaferri, S., 2011. Growth and Demise of Cold Water Coral Ecosystems on Mud Volcanoes in the West Alboran Sea: The Messages from the Planktonic and Benthic Foraminifera. Mar. Geol. 282 (1–2), 26–39.

Martín-Puertas, C., Jimenez Espejo, F., Martinez-Ruiz, F., Nieto-Moreno, V., Rodrigo, M., Mata, M.P., Valero-Garcés, B.L., 2010. Late Holocene climate variability in the southwestern Mediterranean region: an integrated marine and terrestrial geochemical approach. Clim. Past. 6, 807–816.

Morel, J.-L., 1989. États de contrainte et cinématique de la chaîne Rifaine, Maroc, du Tortonien à l'Actuel. Geodin. Acta. 3 (4), 283–294.

Mount, J., 1985. Mixed siliciclastic and carbonate sediments: a proposed first order textural and compositional classification. Sedimentology 32 (3), 435–442.

Nesbitt, H.W., Young, G.M., 1982. Prediction of some weathering trends of plutonic and volcanic rocks based on thermodynamic and kinetic considerations. Geochim. Cosmochim. Acta. 48 (7), 1523–1534.

Nieto-Moreno, V., Martinez-Ruiz, F., Giralt, S., Jimenez Espejo, F., Gallego-Torres, D., Rodrigo-Gamiz, M., García-Orellana, J., Ortega-Huertas, M., de Lange, G.J., 2011. Tracking climate variability in the western Mediterranean during the Late Holocene: a multiproxy approach. Clim. Past. 7, 1395–1414.

Parilla, G., Kinder, T.H., Preller, R.H., 1986. Deep and intermediate Mediterranean Water in the western Alboran Sea. Deep Sea Res. 33 (1), 55–88.

Prieur, L., Sournia, A., 1994. Almofront 1 April–May 1991: An interdisciplinary study of the Almeria–Oran geostrophic front SW Mediterranean Sea. J. Mar. Syst. 5 (3–5), 187–203.

Riding, R., 2002. Structure and composition of organic reefs and carbonate mud mounds: Concepts and categories. Earth-Sci. Rev. 58 (1), 163–231.

Rohling, E.J., Den Dulk, M., Pujol, C., Vergnaud Grazzini, C., 1995. Abrupt hydrographic change in the Alboran Sea western Mediterranean around 8000 yrs BP. Deep Sea Res. Part I 42, 1609–1619.

Sarhan, T., Lafuente, J.G., Vargas, M., Vargas, J.M., Plaza, F., 2000. Upwelling mechanisms in the northwestern Alboran Sea. J. Mar. Syst. 23, 317–331.

Schönwiese, C., 1995. Klimaänderungen: Daten, Analysen, Prognosen. Springer, Heidelberg, Germany.

Schröder-Ritzrau, A., Frank, N., Fohlmeister, J., Waldner, A., Reith, S., 2015. Holocene coral presence across the Strait of Gibraltar MD194 Eurofleets. In: Van Rooij, D., Hamouni, N., Rüggeberg, A. (Eds.), Late Pleistocene Carbonate Mound Record along the Mediterranean Atlantic Gateway. First MD194 EuroFLEETS Gateways post cruise meeting, 5 May 2015. Faculty of Sciences Rabat, Morocco, (Programme and Abstract Book), pp. 10–11.

Stalder, C., Vertino, A., Rosso, A., Rüggeberg, A., Pirkenseer, C., Spangenberg, J.E., Spezzaferri, S., Camozzi, O., Rappo, S., Hajdas, I., 2015. Microfossils, a Key to Unravel Cold Water Carbonate Mound Evolution through Time: Evidence from the Eastern Alboran Sea. PLoS One 10 (10), e0140223.

Suttner, L.J., Dutta, P.K., 1986. Alluvial sandstone composition and paleoclimate, I Framework mineralogy. J. Sediment. Petrol. 56 (3), 329–345.

Tesson, M., Gensous, B., 1978. Les sédiments superficiels de la lagune de Nador (sebkha de Bou Areg) : principales caractéristiques and répartition. Bull. Inst. Pêches Maroc 24.

Titschack, J., Fink, H.G., Baum, D., Wienberg, C., Hebbeln, D., Freiwald, A., 2016. Mediterranean Cold Water Corals: An Important Regional Carbonate Factory? The Depositional Record 2 (1), 74–96.

Van Rooij, D., Hebbeln, D., Comas, M., Vandorpe, T., Delivet, S., 2013. The MD194 shipboard scientists, 2013. EuroFLEETS Cruise Summary. Report «MD194 GATEWAY». Cádiz, Spain, Lisbon, Portugal, 10–21 June. Ghent University, Belgium214.

Vázquez, J.T., Estrada, F., Vegas, R., Ercilla, G., d'Acremont, E., Fernández-Salas, L.M., Alonso, B., Fernández-Puga, M.C., Gomez-Ballesteros, M., Gorini, C., 2014. Quaternary tectonics influence on the Adra continental slope morphology (Northern Alboran Sea). In: Una aproximación multidisciplinar al estudio de las fallas activas, los terremotos y el riesgo sísmic, 2a Reunión Ibérica sobre Fallas Activas y Paleosismología, 22–24 October 2014, Lorca, Spain. 89–92.

Wengler, L., Vernet, J.-L., Ballouche, A., Damblon, F., Michel, P., 1992. Signification des paléomilieux et évolution du climat au Maghreb. Le Maroc oriental au Pléistocène récent. Bull. Soc. Bot. France. Acta. Bot. 139 (2–4), 507–529.

Wienberg, C., Hebbeln, D., Fink, H.G., Mienis, F., Dorschel, B., Vertino, A., López Correa, M., Freiwald, A., 2009. Scleractinian cold-water corals in the Gulf of Cádiz – First clues about their spatial and temporal distribution. Deep Sea Res. Part I Oceanogr. Res. Pap. 56 (10), 1873–1893.